New Phytologist

Research

A role for calcium-dependent protein kinases in differential CO_2- and ABA-controlled stomatal closing and low CO_2-induced stomatal opening in Arabidopsis

Sebastian Schulze[1], Guillaume Dubeaux[1], Paulo H. O. Ceciliato[1], Shintaro Munemasa[2], Maris Nuhkat[3], Dmitry Yarmolinsky[3], Jaimee Aguilar[1], Renee Diaz[1], Tamar Azoulay-Shemer[1,4], Leonie Steinhorst[5], Jan Niklas Offenborn[5], Jörg Kudla[5], Hannes Kollist[3] and Julian I. Schroeder[1]

[1]Division of Biological Sciences, Cell and Developmental Biology Section, University of California San Diego, La Jolla, CA 92093-0116, USA; [2]Graduate School of Environmental and Life Science, Okayama University, Tsushima-Naka, Okayama 700-8530, Japan; [3]Plant Signal Research Group, Institute of Technology, University of Tartu, Nooruse 1, Tartu 50411, Estonia; [4]Fruit Tree Sciences, The Volcani Center, Newe Ya'ar Research Center, Agricultural Research Organization (ARO), Ramat Yishay, Israel; [5]Institute of Plant Biology and Biotechnology, University of Münster, Münster 48149, Germany

Author for correspondence:
Julian I. Schroeder
Email: jischroeder@ucsd.edu

Received: *4 June 2020*
Accepted: *2 November 2020*

New Phytologist (2021) **229:** 2765–2779
doi: 10.1111/nph.17079

Key words: abscisic acid (ABA), *Arabidopsis*, calcineurin B-like proteins (CBLs), calcium, calcium-dependent protein kinases (CPKs), carbon dioxide (CO_2), gas exchange, guard cells.

Summary

- Low concentrations of CO_2 cause stomatal opening, whereas [CO_2] elevation leads to stomatal closure. Classical studies have suggested a role for Ca^{2+} and protein phosphorylation in CO_2-induced stomatal closing. Calcium-dependent protein kinases (CPKs) and calcineurin-B-like proteins (CBLs) can sense and translate cytosolic elevation of the second messenger Ca^{2+} into specific phosphorylation events. However, Ca^{2+}-binding proteins that function in the stomatal CO_2 response remain unknown.
- Time-resolved stomatal conductance measurements using intact plants, and guard cell patch-clamp experiments were performed.
- We isolated *cpk* quintuple mutants and analyzed stomatal movements in response to CO_2, light and abscisic acid (ABA). Interestingly, we found that *cpk3/5/6/11/23* quintuple mutant plants, but not other analyzed *cpk* quadruple/quintuple mutants, were defective in high CO_2-induced stomatal closure and, unexpectedly, also in low CO_2-induced stomatal opening. Furthermore, K^+-uptake-channel activities were reduced in *cpk3/5/6/11/23* quintuple mutants, in correlation with the stomatal opening phenotype. However, light-mediated stomatal opening remained unaffected, and ABA responses showed slowing in some experiments. By contrast, CO_2-regulated stomatal movement kinetics were not clearly affected in plasma membrane-targeted *cbl1/4/5/8/9* quintuple mutant plants.
- Our findings describe combinatorial *cpk* mutants that function in CO_2 control of stomatal movements and support the results of classical studies showing a role for Ca^{2+} in this response.

Introduction

Stomatal pores are formed by pairs of guard cells on the leaf surface. These pores control CO_2 uptake into leaves for photosynthesis while avoiding excessive transpirational water loss. Stomatal apertures are influenced by several environmental factors. Reduced CO_2 concentration ([CO_2]) in the intercellular space of leaves (C_i), high relative humidity, and blue and red light trigger stomatal opening (Mott, 1988; Shimazaki *et al.*, 2007). Stomatal closure on the other hand is triggered by abscisic acid (ABA), darkness, low relative humidity and increased [CO_2] (Kollist *et al.*, 2014; Murata *et al.*, 2015). Changes in the concentration of osmotically active solutes and ions drive osmotic water uptake or efflux from guard cells, thereby regulating the stomatal aperture (Shimazaki *et al.*, 2007; Murata *et al.*, 2015).

Classical studies have provided initial evidence that CO_2-induced stomatal closure is Ca^{2+}-dependent (Schwartz, 1985; Schwartz *et al.*, 1988) and that high [CO_2] itself triggers an elevation in cytosolic free Ca^{2+} concentration ($[Ca^{2+}]_{cyt}$) in guard cells prior to stomatal closure (Webb *et al.*, 1996). Elevated $[Ca^{2+}]_{cyt}$ activates slow-type (S-type) anion efflux channels and vacuolar K^+ efflux channels (VK channels/TPK), while downregulating inward-rectifying K^+ channels and proton pumps in the plasma membrane of guard cells (Schroeder & Hagiwara, 1989; Ward & Schroeder, 1994; Kinoshita *et al.*, 1995; Grabov & Blatt, 1997;

Gobert *et al.*, 2007; Siegel *et al.*, 2009). These responses drive turgor reduction and stomatal closure.

Other studies have indicated that Ca^{2+} is also involved in stomatal opening (Shimazaki *et al.*, 1992; Cousson & Vavasseur, 1998; Young *et al.*, 2006). Repetitive 'spontaneous' $[Ca^{2+}]_{cyt}$ transients were present in guard cells during exposure to low $[CO_2]$, which causes stomatal opening (Young *et al.*, 2006). These Ca^{2+} transients were linked to the more negative plasma membrane potential of guard cells that is required for stomatal opening (Young *et al.*, 2006). Furthermore, experimentally repressed $[Ca^{2+}]_{cyt}$ transients led to attenuated stomatal closure and attenuated stomatal opening in response to elevated or lowered $[CO_2]$, respectively (Young *et al.*, 2006). However, no mutants in Ca^{2+}-binding proteins have been shown to impair CO_2-regulated stomatal responses to date.

In plants, there are several classes of Ca^{2+}-binding sensory proteins, including calmodulins, calcineurin B-like (CBL) proteins and calcium-dependent protein kinases (CPKs) (Sheen, 1996; Cheng *et al.*, 2002). The Arabidopsis genome encodes 10 CBLs and 34 CPKs, which fulfill diverse functions in response to abiotic and biotic stresses (Kudla *et al.*, 1999; Shao & Harmon, 2003; Boudsocq *et al.*, 2010; Reddy *et al.*, 2011; Liu *et al.*, 2017; Yip Delormel & Boudsocq, 2019). Studies have shown a role for calcium-dependent protein kinases in signal transduction and ion-channel regulation in guard cells (Mori *et al.*, 2006; Zhu *et al.*, 2007; Geiger *et al.*, 2010; Brandt *et al.*, 2015). In particular, the roles of CPKs during ABA-induced ion channel regulation have been studied extensively (Mori *et al.*, 2006; Geiger *et al.*, 2010; Brandt *et al.*, 2015; Chen *et al.*, 2019; Zhang *et al.*, 2020). However, the Ca^{2+}-binding proteins that function in CO_2-regulated stomatal movements have remained unknown. Moreover, whether CPKs and/or CBLs function in CO_2-mediated stomatal movements is yet to be investigated, as functional studies are probably hampered by genetic functional redundancy (i.e. overlapping roles) of CPKs and CBLs.

Here we investigate whether CPKs or CBLs are required during CO_2-induced stomatal movements. We generated *cpk* quintuple mutants by crossing *cpk3/4/6/11* and *cpk5/6/11/23* quadruple mutants (Brandt *et al.*, 2015; Li *et al.*, 2018) and analyzed their stomatal response to imposed shifts in $[CO_2]$. We found that neither the progenitor *cpk5/6/11/23* quadruple nor the resulting *cpk3/4/5/6/11* quintuple mutant plants exhibited altered CO_2-dependent stomatal movements. However, we showed that CO_2-controlled stomatal opening and closing were both clearly impaired in *cpk3/5/6/11/23* quintuple mutant plants. The slowing of stomatal opening at low $[CO_2]$ in *cpk3/5/6/11/23* quintuple mutant plants was further investigated. Whole-cell patch-clamp analyses revealed that K^+_{in} channel activity was strongly reduced in *cpk3/5/6/11/23* quintuple mutant guard cells compared to wild-type guard cells. Disruption of plasma membrane mediated CBL signaling in a *cbl1/4/5/8/9* quintuple mutant (Chu *et al.*, 2021) did not clearly affect the kinetics of CO_2-regulated gas exchange. Together, our data suggest important functions of calcium-dependent protein kinases in CO_2-controlled stomatal movements.

Materials and Methods

Plant material and growth conditions

The *Arabidopsis thaliana* accession Columbia (Col-0) was used throughout this study. Seeds were surface sterilized using vapor-phase sterilization, and incubated for 3–4 h in a sealed desiccator with a flask containing 100 ml bleach, to which 5 ml 12.1 N HCl was added. Sterilized seeds were transferred to ½ Murashige & Skoog (½MS) medium (pH 5.8) supplemented with 0.8% phyto-agar and stratified for 2 d at 4°C in the dark. Plates with seeds were then incubated for 7 d at 80 μmol m^{-2} s^{-1} light intensity with a 12 h : 12 h, light : dark photoperiod, at 21°C and 40–50% relative humidity for 7 d. Seedlings were transplanted to soil-containing pots (Sunshine Mix #1, Sungro Horticulture, Agawam, MA, USA) and were grown in a growth chamber (Conviron, Winnipeg, Manitoba, Canada) under a 12 h : 12 h, light : dark photoperiod, at a light intensity of *c.* 150 μmol m^{-2} s^{-1}, a temperature of 21°C and a relative humidity of 50–60% (at University of California, San Diego, CA, USA).

In Tartu (Estonia) all plants were grown in soil mix containing 2 : 1 (v/v) peat and vermiculite. Arabidopsis plants were cultivated in growth chambers (MCA1600, Snijders Scientific, Tilburg, the Netherlands) at a 12 h photoperiod, 150 μmol m^{-2} s^{-1} light intensity, 23°C : 18°C, day : night temperature and 70% relative humidity. The plants were grown through openings in glass plates which prevented the water vapor from the soil from reaching the leaf cuvettes of the gas-exchange analyzer. Holes in the glass plates were closed with pruning wax 3–4 d before the experiments.

Mutant lines of *cpk3/4/5/6/11* and *cpk3/5/6/11/23* were generated through crossing *cpk3/4/6/11* (Li *et al.*, 2018) and *cpk5/6/11/23* (Brandt *et al.*, 2015). Oligonucleotides used for genotyping higher order *cpk* mutant lines (Supporting Information Fig. S2) are given Table S1.

The generation of the *cbl1/4/5/8/9* quintuple mutant has been described previously (Chu *et al.*, 2021).

Time-resolved stomatal conductance measurements

Intact leaves of 4- to 5-wk-old Arabidopsis plants were used for time-resolved stomatal conductance (gs) measurements using LI-6400 and LI-6400XT infrared-based gas exchange analyzer (IRGA) systems with a leaf chamber (Li-Cor Biosciences, Lincoln, NE, USA) at UC San Diego. For analyses of CO_2-dependent stomatal conductance measurements, clamped leaves attached to intact plants were equilibrated and stabilized at 150 μmol m^{-2} s^{-1} light intensity (6400-02B LED light source), at 60–65% relative humidity, 21°C, 360 ppm or 400 ppm $[CO_2]$ and with an incoming air flow of 200 μmol s^{-1} for 1 h. After stomatal conductance stabilized, it was then recorded for 30 min at 360 ppm or 400 ppm $[CO_2]$, followed by 1 h at 800 ppm $[CO_2]$ and 1 h at 100 ppm $[CO_2]$. Stomatal conductance measurements in response to 2 μM ABA or 0.7 μM ABA were carried out with detached intact leaves in which ABA was added to the transpiration stream via the petiole, as described previously (Ceciliato *et al.*, 2019). For light response measurements, whole

plants were kept in the dark for 18 h before analysis. After stabilization of gs for 45–60 min, stomatal conductance of individual intact leaves was measured for 10 min in the dark, followed by red light (600 µmol m^{-2} s^{-1}) exposure for 30 min. After red light treatment, blue light (10 µmol m^{-2} s^{-1}) was applied and superimposed on red light, and stomatal conductance was measured for another 30 min as described previously (Shimazaki *et al.*, 2007; Hauser *et al.*, 2019).

Whole plant rosette stomatal conductance responses were measured in an eight-chamber gas-exchange device in Tartu, Estonia, as described by Kollist *et al.* (2007). Arabidopsis plants (3–4-wk old) were inserted into the device and incubated 1 h for stabilization of stomatal conductance. Standard conditions in the chambers were as follows: ambient CO_2 (400 ppm), 150 µmol m^{-2} s^{-1} light intensity, *c.* 70% relative humidity, 24°C. Stomatal responses to shifts in [CO_2] were recorded for 1 h at 800 ppm or 100 ppm [CO_2], respectively.

Biological variation of steady-state baseline stomatal conductance occurs in Arabidopsis among plants grown at different times (Zhang *et al.*, 2018a,b). Therefore, in the experiments wild-type and mutant plants were grown side by side and analyzed in the same time period. Furthermore, gas exchange experimental datasets were repeated in independent runs at different times of the year. In each independent set of experiments, $n \geq 3$ intact leaves, intact leaves attached to whole plant rosettes, or intact whole plant rosettes per genotype were analyzed.

Curve fitting and quantifications of stomatal conductance responses

The PYTHON programming language and multiple software packages were used to quantify the stomatal conductance responses described throughout this article (Figs 1, 2, S6). Comma-separated values (CSV) files detailing stomatal closure and opening responses were first imported in independent NUMPY arrays (https://numpy.org). This simplified curve-fit function was then imported from SCIPY (https://scipy.org). The following one-phase decay equation was used to test and obtain fitted curves for stomatal closure responses: $y = (y_0 - \text{plateau}) \cdot e^{-Kx} + \text{plateau}$, where y_0 is the stomatal conductance just before the application of the stimulus (high CO_2 800 ppm); plateau is the predicted stomatal conductance at infinite times; K is the rate constant, expressed in s^{-1}; and τ is the time constant, expressed in s, which is the reciprocal of K, such that $\tau = 1/K$. For stomatal closure responses, the amplitude was calculated as follows: amplitude a $= y_0 -$ plateau. Curve fitting for stomatal opening traces was calculated with a different one-phase association equation: $y = y_0 + (\text{plateau} - y_0) \cdot (1 - e^{-Kx})$. For stomatal opening responses, the amplitude was calculated as follows: amplitude = plateau $- y_0$. Means of stomatal opening or closure response traces together with their corresponding fitted curves were plotted using MATPLOTLIB (https://matplotlib.org). The means ± SD of τ and amplitude were plotted for the different genotypes. For each curve fitting plot, *t*-tests were used to determine whether the mean of τ and amplitude were significantly different between genotypes (i.e. between wild-type and *cpk* mutants). Detailed PYTHON scripts are available upon request.

Stomatal index and density assays

Stomatal index and density were analyzed in 4- to 5-wk-old Arabidopsis plants as described previously (Azoulay-Shemer *et al.*, 2015). The 5th true leaves of individual plants were cleared in an ethanol : acetic acid solution (7 : 1 (v/v)). Cleared leaves were

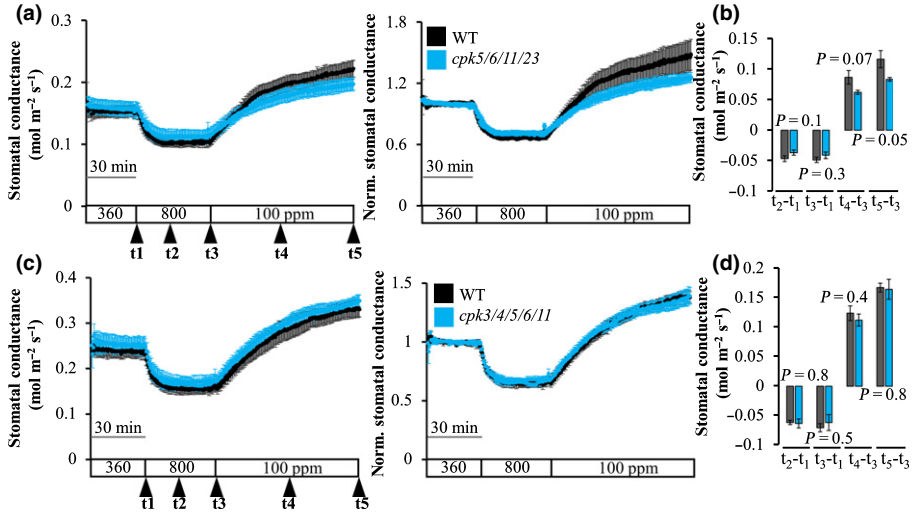

Fig. 1 Stomata of (a, b) *cpk5/6/11/23* quadruple mutant and (c, d) *cpk3/4/5/6/11* quintuple mutant leaves respond to shifts in imposed ambient [CO_2] similarly to wild-type leaves. The graphs show average stomatal conductance (± SE) of wild-type (WT, Col-0) and (a) *cpk5/6/11/23* quadruple mutant ($n = 4$ independent leaves per genotype) or (c) *cpk3/4/5/6/11* quintuple mutant leaves ($n = 5$ independent leaves per genotype) in response to imposed shifts in air CO_2 concentrations (as indicated on the *x*-axis; ppm). Stomatal conductance data (left panel) were normalized to the average of the first 30 min of stomatal conductance values at 360 ppm [CO_2]. (b, d) Changes in absolute stomatal conductance (mean ± SE) were calculated at the indicated time points (t_1, shift to 800 ppm [CO_2]; t_2, 10 min after shift to 800 ppm [CO_2]; t_3, shift to 100 ppm [CO_2]; t_4, 45 min after shift to 100 ppm [CO_2]; t_5 , final measurement). One-way ANOVA was used for statistical tests. See Supporting Information Figs S1 and S3 for curve fitting analyses. Two (a) and three (c) independent sets of experiments conducted at different times showed similar results to those shown here.

softened in 1 M KOH for 20–30 min and rinsed twice with deionized water. Midveins were removed, and a small leaf area was excised from the center of each leaf blade away from the margins and mounted on 15% glycerol. Four images of the abaxial side of each sample were randomly taken using a differential interference contrast (DIC) microscope (Leica DM5000 B (Leica Microsystems Inc., Buffalo Grove, IL, USA) mounted with a 15.2 mM 64 Mp shifting pixel camera (Diagnostic Instruments Inc., Sterling Heights, MI,USA)). In total, eight images were taken per individual plant, with nine plants per genotype (i.e. 72 images). Stomata and pavement cells were quantified using ImageJ (https://imagej.nih.gov/ij/). Stomatal index was calculated by dividing the number of stomata by the total number of cells (stomata + pavement cells). All analyses were carried out in genotype-blinded assays.

Patch-clamp recordings

Arabidopsis guard cell protoplasts were prepared as previously described (Laanemets *et al.*, 2013; Brandt *et al.*, 2015). Two rosette leaves were blended. Epidermal tissues were collected using a 100 µm nylon mesh and incubated in 10 ml digestion solution (1% (w/v) cellulase R10 (Yakult Pharmaceutical Industry, Tokyo, Japan), 0.5% (w/v) macerozyme R10 (Yakult Pharmaceutical Industry, Tokyo, Japan), 500 mM D-mannitol, 0.5% (w/v) BSA, 0.1% (w/v) kanamycin sulfate, 10 mM ascorbic acid, 0.1 mM KCl, and 0.1 mM $CaCl_2$) at 25°C for 16 h on a circular shaker at 50 rpm. The digestion mixture was filtered through a 10 µm nylon mesh. Guard cell protoplasts were washed twice with wash solution (500 mM D-sorbitol, 0.1 mM $CaCl_2$, 0.1 mM KCl, pH 5.6) by centrifugation at 200 ***g*** for 5 min at room temperature. Isolated guard cell protoplasts were kept on ice before use.

Inwardly rectifying K^+ (K^+_{in}) channel currents were recorded with an Axon 200A amplifier (Molecular Devices, San Jose, CA, USA) and a Digidata 1440A digitizer (Molecular Devices, San Jose, CA, USA). K^+_{in} pipette solution contained 70 mM K-Glutamate, 30 mM KCl, 2 mM $MgCl_2$, 3.35 mM $CaCl_2$, 6.7 mM EGTA, 10 mM HEPES-Tris (pH 7.1), and 5 mM Mg-ATP. The osmolality of the K^+_{in} pipette solution was adjusted to 500 mmol kg^{-1} with D-sorbitol. K^+_{in} bath solution contained 30 mM KCl, 2 mM $MgCl_2$, 1 mM $CaCl_2$, and 10 mM MES-Tris (pH 5.5). The osmolality of the K^+_{in} bath solution was adjusted to 485 mmol kg^{-1} with D-sorbitol. The free $[Ca^{2+}]_{cyt}$ was calculated at *c.* 290 nM using the web-based WebmaxC calculator (https://somapp.ucdmc.ucdavis.edu/pharmacology/bers/maxchelator/webmaxc/webmaxcS.htm).

Results

CO_2-induced stomatal movements are defective in *cpk3/5/6/11/23* quintuple mutant plants

To investigate whether CPKs function in CO_2-mediated stomatal movements, stomatal conductance responses of 5-wk-old leaves attached to intact plants from *cpk* T-DNA mutants were analyzed. The quadruple mutant *cpk5/6/11/23* (Brandt *et al.*, 2015) responded to shifts in $[CO_2]$ similarly to leaves of wild-type (Col-0) plants (Fig. 1a). Differences in stomatal conductance during high CO_2-induced stomatal closure and low CO_2-mediated stomatal opening were similar between the wild-type and mutant plants (one-way ANOVA, $P = 0.3$ and $P = 0.05$, respectively; Fig. 1b). Fitted curves were calculated for stomatal opening and closure traces and compared between wild-type and the *cpk5/6/11/23* quadruple mutant, showing similar time constants for average stomatal closing and opening kinetics (Fig. S1b,c; $P = 0.4$ and $P = 0.6$ for stomatal closing and opening, respectively).

Possible involvement of CPKs in CO_2-mediated stomatal movements might not become visible due to functional redundancy (Yip Delormel & Boudsocq, 2019). For instance, CPK5 and CPK6, as well as CPK4 and CPK11, are closely related, indicating a possible overlap in function (Boudsocq & Sheen, 2013). We therefore generated the two *cpk* quintuple mutants *cpk3/4/5/6/11* and *cpk3/5/6/11/23* by crossing *cpk3/4/6/11* (Li *et al.*, 2018) with *cpk5/6/11/23* (Brandt *et al.*, 2015) (Fig. S2; Table S1). Neither *cpk3/4/5/6/11* nor *cpk3/5/6/11/23* quintuple mutant plants displayed any obvious growth phenotypes in growth chambers under nonstress growth conditions after 4–5 wk of growth. We analyzed the stomatal conductance responses of these homozygous quintuple mutants using infrared gas exchange analyzers. Leaves attached to intact plants of *cpk3/4/5/6/11* quintuple mutant plants responded to shifts from ambient (360 ppm) to high (800 ppm) $[CO_2]$ with rapid and robust stomatal closure (Fig. 1c). Shifts from high (800 ppm) to low (100 ppm $[CO_2]$) induced robust stomatal opening (Fig. 1c). These CO_2 responses of *cpk3/4/5/6/11* quintuple mutant plants were comparable to wild-type control plants (Fig. 1d; one-way ANOVA, $P = 0.5$ (stomatal closure) and $P = 0.8$ (stomatal opening)). Fitted curves were calculated for stomatal opening and closure traces for the wild-type and *cpk3/4/5/6/11* quintuple mutants, and their comparison showed similar time constants (Fig. S3; $P = 0.9$ and $P = 0.3$ for stomatal closing and opening, respectively).

Independent studies carried out under different growth conditions with whole intact plants in the laboratory of H. Kollist (in Tartu, Estonia) confirmed that *cpk3/4/5/6/11* quintuple mutant plants displayed intact high $[CO_2]$-induced stomatal closing (Fig. S4a,b; $P = 0.8$) and low $[CO_2]$-mediated stomatal opening (Fig. S4c,d; $P = 0.35$).

Interestingly, in contrast to the *cpk5/6/11/23* quadruple and *cpk3/4/5/6/11* quintuplemutant lines, *cpk3/5/6/11/23* quintuple mutant plants displayed slower CO_2 responses to shifts from ambient (400 ppm) to high (800 ppm) $[CO_2]$ (Fig. 2a). The average absolute decrease in stomatal conductance in the *cpk3/5/6/11/23* quintuple mutant clearly differed from wild-type 10 min after the shift to 800 ppm $[CO_2]$ (Fig. 2b; $P = 0.01$; Fig. S5a). Unexpectedly, leaves of these *cpk3/5/6/11/23* plants also responded with substantially slower stomatal opening in response to low $[CO_2]$ (100 ppm) compared with wild-type plants (Figs 2a, S5b). In this study, the average absolute increase in stomatal conductance was lower compared to wild-type 45 min after shifting to high $[CO_2]$ (Fig. 2b; $P = 0.01$). Despite clearly

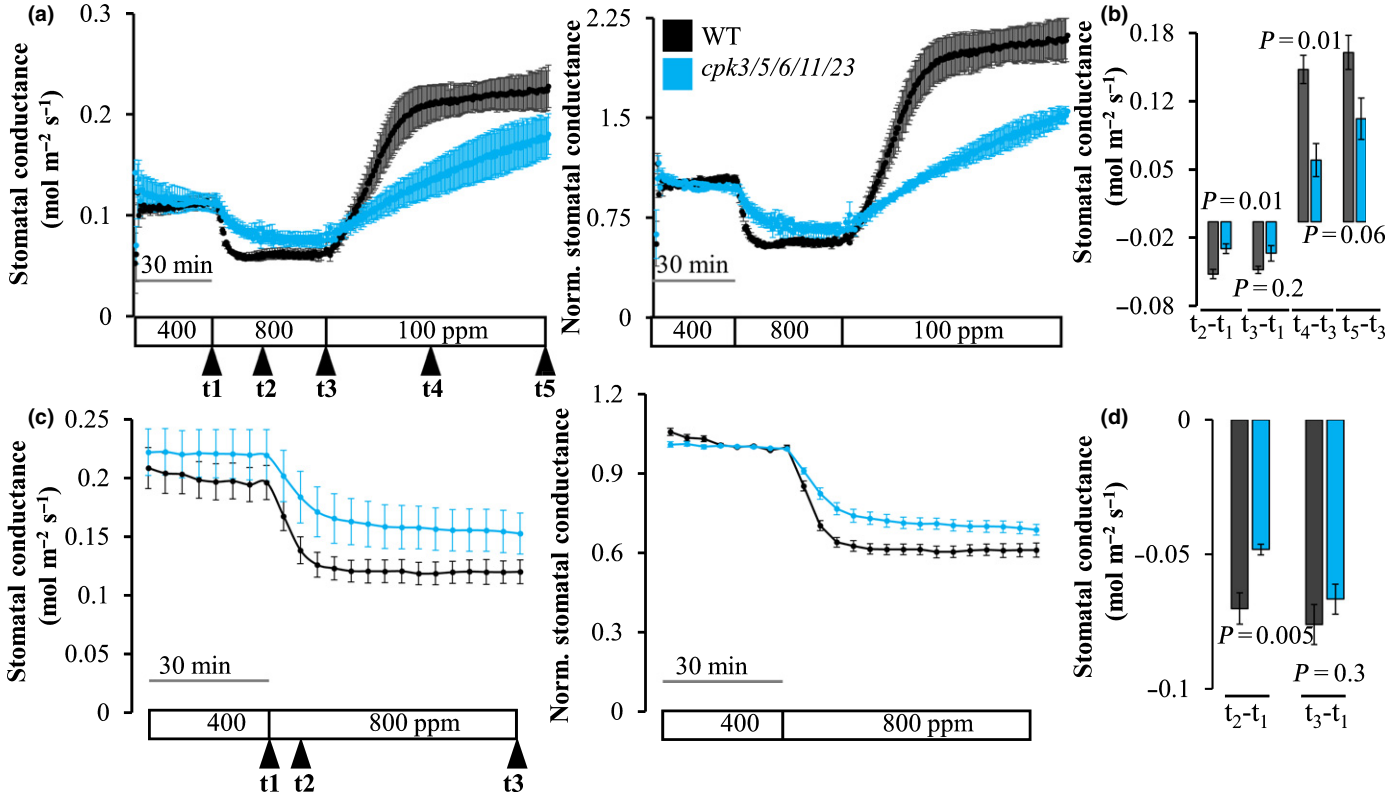

Fig. 2 Intact leaves and whole plant rosettes of *cpk3/5/6/11/23* quintuple mutant plants show altered stomatal opening and closure responses to shifts in ambient CO_2 concentrations. (a) The graphs show average stomatal conductance ± SE in response to imposed shifts in ambient CO_2 concentrations (as indicated on the *x*-axis; ppm) of wild-type (WT, Col-0, $n = 3$ independent leaves) and *cpk3/5/6/11/23* quintuple mutant plants ($n = 4$ independent leaves). Stomatal conductance (left panel) was normalized to the average of the first 30 min of stomatal conductance values at 400 ppm [CO_2] (right panel). See Supporting Information Fig. S4 for curve fitting and statistical analyses. (b) Changes in absolute stomatal conductance (mean ± SE) were calculated at the indicated time points (t_1, shift to 800 ppm [CO_2]; t_2, 10 min after shift to 800 ppm [CO_2]; t_3, shift to 100 ppm [CO_2]; t_4, 45 min after shift to 100 ppm [CO_2]; t_5, final measurement). (c) Stomatal conductance responses to imposed shifts in ambient CO_2 concentrations (as indicated on the *x*-axis; ppm) in whole plant rosettes (mean ± SE) of wild-type (WT, Col-0) and *cpk3/5/6/11/23* quintuple mutant plants ($n = 6$ independent whole rosettes per genotype). Stomatal conductance (left panel) was normalized to the average of 15 min of stomatal conductance values at 400 ppm [CO_2] (right panel). Experiments and data analyses in (c) were carried out genotype blinded. (d) Changes in absolute stomatal conductance (mean ± SE) were calculated at the indicated time points (t_1, shift to 800 ppm [CO_2]; t_2, 12 min after shift to 800 ppm [CO_2]; t_3, final measurement). Despite clearly slowed stomatal kinetics (see the Results section), stomatal conductances reached similar values at the end of exposures (b, d). One-way ANOVA was used for statistical tests. (a, c) Three independent sets of experiments, each conducted at different times, showed similar results to those shown here (see Figs S4 and S6, respectively).

slowed stomatal kinetics, stomatal conductance in *cpk3/5/6/11/23* quintuple mutant leaves eventually reached values similar to wild-type at the end of exposures in these experiments (Fig. 2b; stomatal closing $P = 0.2$; stomatal opening $P = 0.06$). These findings were reproducibly observed in three independent experimental data sets, with each experimental set analyzing ≥3 independent mutant plants (e.g. Fig. S6). We also plotted net assimilation rates of intact *cpk3/5/6/11/23* quintuple mutant leaves in response to shifts in [CO_2] (Fig. S6c). The data indicate that steady-state assimilation rates were relatively similar to assimilation rates measured in wild-type leaves and therefore not strongly affected in *cpk3/5/6/11/23* quintuple mutant plants under the imposed conditions.

Further, independent genotype blind studies were carried out under different growth conditions with whole intact plants of these lines in the laboratory of H. Kollist. In these genotype blinded experiments, *cpk3/5/6/11/23* quintuple mutant plants showed a similar tendency of slowed and impaired stomatal closure in response to [CO_2] elevation (800 ppm; Figs 2c, S4a). Shifts to low [CO_2] (100 ppm) displayed a less dramatic, reduced average magnitude of stomatal opening in intact *cpk3/5/6/11/23* quintuple mutant whole plant rosettes compared to wild-type controls (Fig. S4c). The average absolute decrease in stomatal conductance in *cpk3/5/6/11/23* quintuple mutant plants differed from wild-type 12 min after the shift to 800 ppm [CO_2] (Fig. 2d; $P = 0.005$). The decrease in absolute stomatal conductance in *cpk3/5/6/11/23* quintuple mutant plants reached values similar to wild-type at the end of the measurement period (Fig. 2d; $P = 0.3$), similar to the earlier 'single-leaf-intact-plant' gas exchange analyses (Fig. 2a, b). Taken together, data from our independent laboratories with different growth conditions using either single-leaf-intact-plants or whole-plant gas exchange analyses show qualitatively similar and reproducible impairments in *cpk3/5/6/11/23* mutant plants in CO_2-induced stomatal closing and stomatal opening (Figs 2, S4).

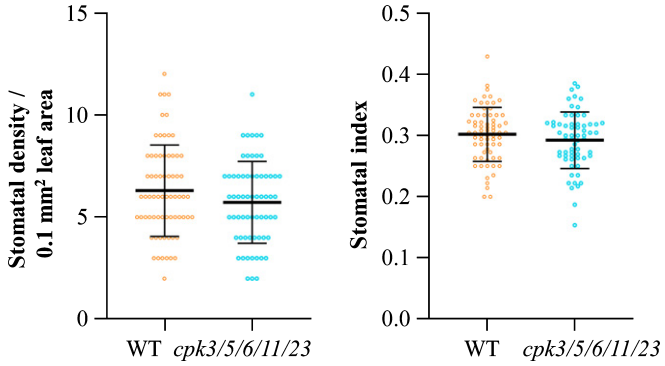

Fig. 3 Stomatal index and density values for *cpk3/5/6/11/23* quintuple mutant leaves are comparable to wild-type. Stomatal density and index values for the abaxial side of the 5th true leaves of wild-type (WT, Col-0) and *cpk3/5/6/11/23* quintuple mutant leaves were determined in genotype-blinded assays. Mean values for $n = 9$ individual plants per genotype, with eight images per plant (± SD) taken with a differential interference contrast (DIC) microscope, are plotted (see the Materials and Methods section for details). Stomatal density and stomatal index were similar for wild-type and *cpk3/5/6/11/23* quintuple mutant leaves (one-way ANOVA $P = 0.124$ and $P = 0.22$, respectively). One representative experimental set of a total of three independently conducted genotype blinded studies with similar findings is shown.

We next conducted experiments to determine whether altered stomatal development was associated with the impaired CO_2-mediated stomatal responses in leaves of *cpk3/5/6/11/23* quintuple mutant plants. We performed stomatal imaging analyses in genotype-blinded studies in true leaves of 4–5 wk-old plants. Our data show that both stomatal density and stomatal index in *cpk3/5/6/11/23* quintuple mutant leaves were comparable to wild-type, suggesting that stomatal development was not altered in *cpk3/5/6/11/23* quintuple mutant leaves (Fig. 3; one-way ANOVA, $P = 0.12$ and $P = 0.22$ for stomatal density and stomatal index, respectively). These results highlight that *cpk3/5/6/11/23* quintuple mutants were defective in CO_2-mediated stomatal movements but stomatal development was not affected.

CO_2-mediated stomatal movements in plasma membrane targeted calcium-sensing CBL protein mutant plants

cpk3/5/6/11/23 quintuple mutant plants showed impaired CO_2-induced stomatal movements (Fig. 2). We investigated whether mutants in other calcium-sensing proteins would show a similar phenotype. Calcium-sensing calcineurin B-like (CBL) proteins play essential roles in ABA and abiotic stress responses (Albrecht *et al.*, 2003; Pandey *et al.*, 2004; Batistič & Kudla, 2009; Mao *et al.*, 2016). Five of the ten CBL proteins encoded in the Arabidopsis genome are targeted to the plasma membrane (Batistič *et al.*, 2008, 2010; Chu *et al.*, 2021). We therefore analyzed CO_2-induced stomatal movements in a quintuple mutant of these plasma membrane-localized CBLs (*cbl1/4/5/8/9*) (Chu *et al.*, 2021). Stomatal conductance analyses of *cbl1/4/5/8/9* quintuple mutant leaves showed intact stomatal closing and opening in response to lowered and elevated [CO_2] in one set of experiments (Fig. 4a,b). Small changes in the amplitude of stomatal closing in response to high [CO_2] were observed in an independent set of experiments (Fig. 4c,d).

Guard cells of *cpk3/5/6/11/23* quintuple mutants show reduced K^+_{in} channel currents

Impairment of low CO_2-mediated stomatal opening in *cpk3/5/6/11/23* quintuple mutant leaves could be mediated by a diverse combination of mechanisms. K^+_{in} channels in guard cells mediate K^+ uptake during stomatal opening and were found to show a reduced Ca^{2+}-dependent activity in *slac1* mutant alleles (Laanemets *et al.*, 2013). The H^+-ATPase located in the guard cell plasma membrane pumps protons from the guard cell cytosol to the cell wall and creates an electrochemical gradient across the plasma membrane (Shimazaki *et al.*, 2007). This membrane hyperpolarization triggers the activation of potassium uptake (K^+_{in}) channels that mediate the uptake of K^+ (Kwak *et al.*, 2001; Lebaudy *et al.*, 2008). We therefore analyzed K^+_{in} channel currents using whole-cell patch-clamp techniques in *cpk3/5/6/11/23* quintuple mutant guard cells. Interestingly, a reduction of K^+_{in} channel activity in *cpk3/5/6/11/23* quintuple mutant guard cell protoplasts was observed compared to wild-type (Fig. 5). The K^+_{in} channel current magnitude at −120 mV and −160 mV was reduced by *c.* 60–69% in *cpk3/5/6/11/23* quintuple mutant guard cells (Fig. 5; one-way ANOVA, $P = 0.04$).

Analyses of stomatal conductance responses to red and blue light in intact leaves

Since *cpk3/5/6/11/23* quintuple mutant leaves exhibited a slowed stomatal opening in response to low [CO_2] (Figs 2a, S6), we analyzed light-dependent stomatal opening in leaves of intact *cpk3/5/6/11/23* quintuple mutant plants by carrying out gas exchange measurements in response to blue and red light. Wild-type and *cpk3/5/6/11/23* quintuple mutant plants were kept in the dark for 18 h before the experiments, and the stomatal conductance of leaves was allowed to settle to stable values. The steady-state stomatal conductance of intact leaves was measured for 10 min prior to light exposure. The average steady state dark-adapted stomatal conductance of *cpk3/5/6/11/23* quintuple mutant leaves was slightly larger than that of wild-type plants before light exposure in some experiments but was within biological variability (Fig. 6a; stomatal conductance (mol m^{-2} s^{-1}) of wild-type: mean = 0.107, SD = 0.038; and *cpk3/5/6/11/23*: mean = 0.134, SD = 0.047; one-way ANOVA $P = 0.4$). After application of red light (600 µmol m^{-2} s^{-1}), stomatal conductance increases were observed for both *cpk3/5/6/11/23* quintuple mutant and wild-type leaves with similar magnitudes and kinetics (Fig. 6; $P = 0.1$). Results from an independent set of experiments are shown in Fig. S7 ($P = 0.7$). Stomatal conductance increased further when blue light (10 µmol m^{-2} s^{-1}) was superimposed on red light. Stomatal opening responses to blue light were comparable in intact leaves of *cpk3/5/6/11/23* quintuple mutant and wild-type plants (Fig. 6; $P = 0.8$ Fig. S7; $P = 0.9$). Thus, *cpk3/5/6/11/23* quintuple mutant leaves exhibited clearly defective stomatal responses to CO_2, whereas light-induced stomatal opening was not clearly affected under the imposed conditions.

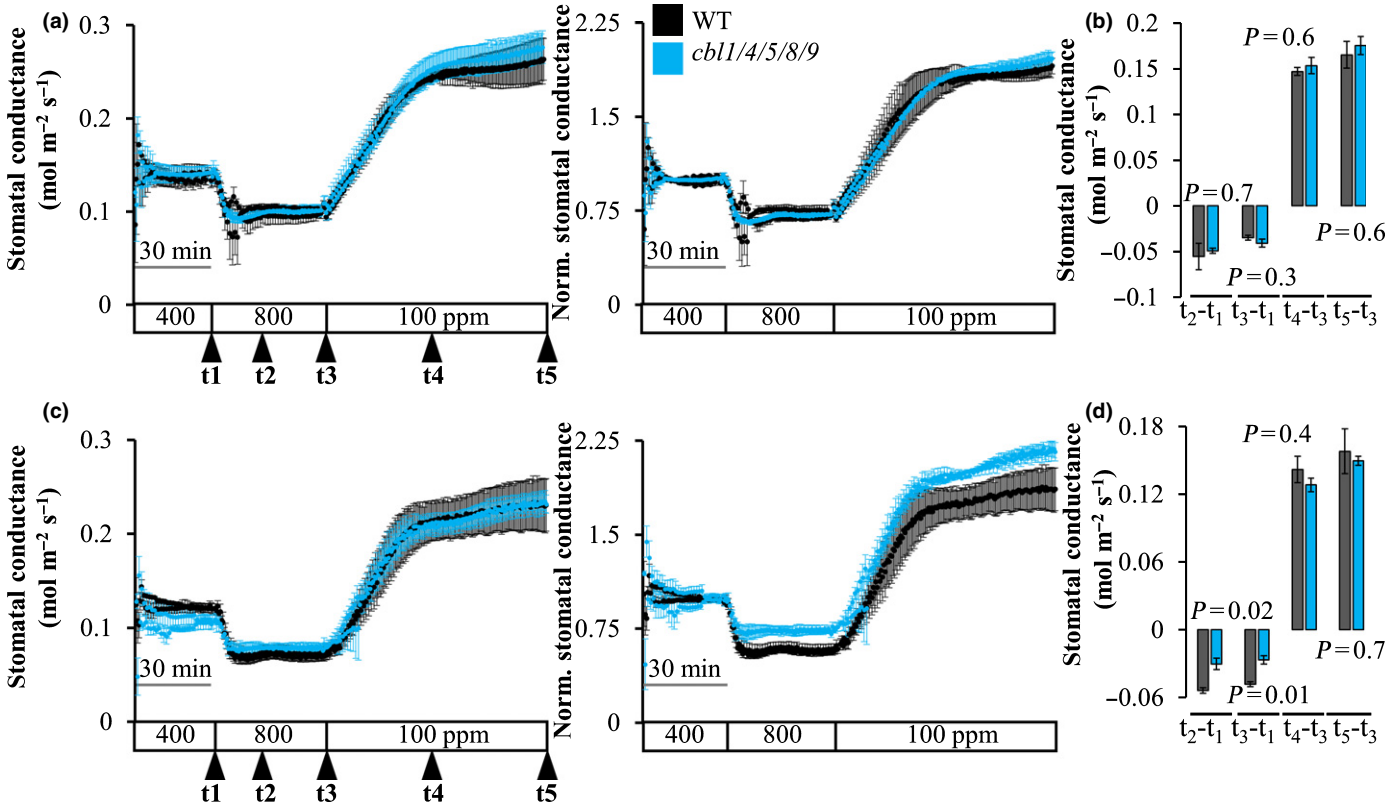

Fig. 4 Stomatal conductance responses in *cbl1/4/5/8/9* quintuple mutant leaves to shifts in imposed ambient [CO_2]. (a, c) Two independent experimental sets are presented. The graphs show the time courses of average stomatal conductance (± SE) responses in wild-type (WT, Col-0) and *cbl1/4/5/8/9* quintuple mutant plants ($n = 3$ independent leaves per genotype in each experimental set) in response to imposed shifts in ambient (air) CO_2 concentrations (as indicated on the *x*-axis; ppm). Stomatal conductances (left panels) were normalized to the average of the first 30 min of stomatal conductance values at 400 ppm [CO_2] (right panels). (b, d) Changes in absolute stomatal conductance are shown. Differences in stomatal conductance (mean ± SE) were calculated at the indicated time points (t_1, shift to 800 ppm [CO_2]; t_2, 10 min after shift to 800 ppm [CO_2]; t_3, shift to 100 ppm [CO_2]; t_4, 45 min after shift to 100 ppm [CO_2]; t_5, final measurement). One-way ANOVA was used for statistical tests.

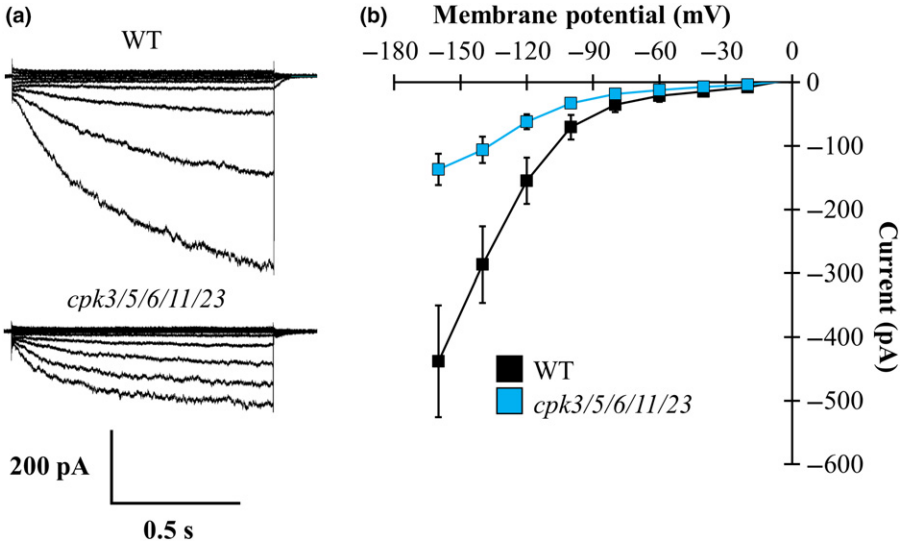

Fig. 5 Inward rectifying K^+ channel activity is decreased in *cpk3/5/6/11/23* quintuple mutant guard cells. (a) Representative current traces of wild-type (WT, Col-0, upper trace) and *cpk3/5/6/11/23* (lower trace) guard cell protoplasts are shown. (b) Average current–voltage relationship curves for WT ($n = 12$) and *cpk3/5/6/11/23* quintuple mutant ($n = 11$) guard cell protoplasts. Error bars represent SEM.

ABA-mediated stomatal closure in *cpk3/5/6/11/23* and *cpk3/4/5/6/11* quintuple mutant leaves

To investigate whether stomatal movements triggered by other stimuli were impaired in intact *cpk3/5/6/11/23* quintuple mutant leaves, ABA-dependent stomatal closure was analyzed by conducting gas-exchange experiments in which ABA was applied to the transpiration stream via the petioles of excised intact leaves (Ceciliato *et al.*, 2019). The magnitude of stomatal closure after application of 2 µM ABA to leaves of *cpk3/5/6/11/23* mutant

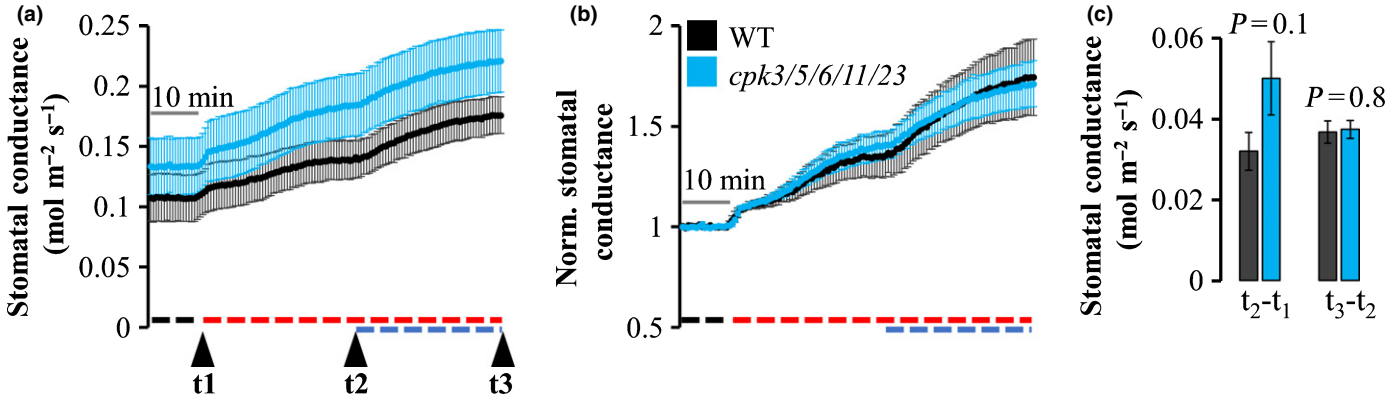

Fig. 6 The function of guard cells of *cpk3/5/6/11/23* quintuple mutant leaves is not impaired in red light and blue light-induced stomatal opening. Stomatal conductance of wild-type (WT, Col-0) and *cpk3/5/6/11/23* quintuple mutant leaves in response to shifts in light quality and quantity (black dashed line, darkness; red dashed line, red light at 600 μmol m^{-2} s^{-1}; blue dashed line, blue light at 10 μmol m^{-2} s^{-1}). Plants were incubated in darkness overnight before measurements. Mean (±SE) of $n = 4$ leaves from individual plants per genotype are shown. (a) Stomatal conductance (left panel) was (b) normalized to the average stomatal conductance values recorded for 10 min in the dark (right panel). (c) Differences in absolute stomatal conductance (mean ± SE) were calculated at the indicated time points (t_1, application of red light; t_2, application of blue light; t_3, final measurement). One-way ANOVA was used for statistical tests. Three independent sets of experiments conducted at different times showed similar results to those shown here (see Supporting Information Fig. S7 for an independent experiment).

plants was variable when compared to responses measured in leaves of wild-type plants grown in parallel (Fig. 7). The degree and time course of stomatal closure in response to ABA application varied between four independent experiments (Fig. 7; $n \geq 3$ mutant leaves analyzed per experimental data set). Leaves of *cpk3/5/6/11/23* quintuple mutant plants showed ABA-dependent stomatal closure that was very similar to that observed in the wild-type in one of the four independent experimental sets (Fig. 7a) and had a similar overall absolute magnitude in another set of experiments (Fig. 7d). Furthermore, reduction in absolute stomatal conductance after application of ABA led to similar values, as shown in Fig. 7(a,d) ($P = 0.6$ and 0.5), but the average absolute steady-state stomatal conductance before ABA application was larger in *cpk3/5/6/11/23* in the later set of experiments, albeit with a 94% confidence interval (Fig. 7d; $P = 0.06$). By contrast, ABA-mediated stomatal closure in *cpk3/5/6/11/23* quintuple mutant leaves was impaired in other experimental sets (Fig. 7b; $P = 0.03$ and Fig. 7c; $P = 0.03$).

We further analyzed stomatal closure responses using a lower ABA concentration of 0.7 μM, applied to the transpiration stream. Our data show variation in *cpk3/5/6/11/23* quintuple mutant responses compared to wild-type responses to 0.7 μM ABA application between three independent sets of experiments (Fig. S8; $n \geq 3$ mutant leaves analyzed per experiment and genotype). ABA-mediated stomatal closure in *cpk3/5/6/11/23* quintuple mutant leaves was slightly impaired in one set of experiments 10 min after application of ABA (Fig. S8a; $P = 0.01$). Stomatal conductance reached values similar to those of wild-type plants by the end of our measurements (Fig. S8a; $P = 0.4$). By contrast, stomatal closure responses mediated by 0.7 μM ABA were comparable between *cpk3/5/6/11/23* quintuple mutant leaves and wild-type in two of three independent experimental sets (Fig. S8b,c).

We pursued similar analyses in quintuple mutant leaves of a different combination of *CPK* genes (*cpk3/4/5/6/11*) to investigate whether stomatal closure, mediated by application of 2 μM ABA, was altered in these mutant plants (Fig. 8). Our results indicate variable stomatal closure responses to 2 μM ABA in three independent experimental sets (Fig. 8a–c). Abscisic acid-induced stomatal closure responses were similar to wild-type in two independent studies (Fig. 8a,c). Contrary to these results, stomatal closure in *cpk3/4/5/6/11* quintuple mutant leaves was clearly slower compared to wild-type in a third experimental set (Fig. 8b: $P = 0.012$). Further, we also analyzed stomatal closure in response to 0.7 μM ABA in three independent experimental sets (Fig. S9). *cpk3/4/5/6/11* quintuple mutant plants showed variable responses to 0.7 μM ABA in our analyses, with a slower response in one of three independent data sets. However, the absolute changes in stomatal conductance did not differ from wild-type in all three experimental sets (Fig. S9).

Thus, *cpk3/5/6/11/23* but not *cpk3/4/5/611* quintuple mutant leaves exhibited defective stomatal responses to changes in [CO_2], whereas ABA-mediated stomatal closure was partially slowed in both *cpk* quintuple mutants in some experiments, while showing variability in gas exchange analyses.

Discussion

Calcium functions in regulating stomatal movements (McAinsh *et al.*, 1990; Grabov & Blatt, 1998; Assmann & Shimazaki, 1999). Involvement of calcium in ABA-mediated stomatal closure has been extensively studied over the last few decades (De Silva *et al.*, 1985; Schwartz, 1985; McAinsh *et al.*, 1990; Grabov & Blatt, 1998; MacRobbie, 2000; Siegel *et al.*, 2009; Geiger *et al.*, 2010; Huang *et al.*, 2019). Some studies also observed a role for Ca^{2+} in stomatal opening (Shimazaki *et al.*, 1992, 2007; Cousson & Vavasseur, 1998; Shimazaki, 1999; Young *et al.*, 2006). A Ca^{2+}-dependence of CO_2-induced stomatal closing has been found (Schwartz, 1985; Schwartz *et al.*, 1988; Webb *et al.*,

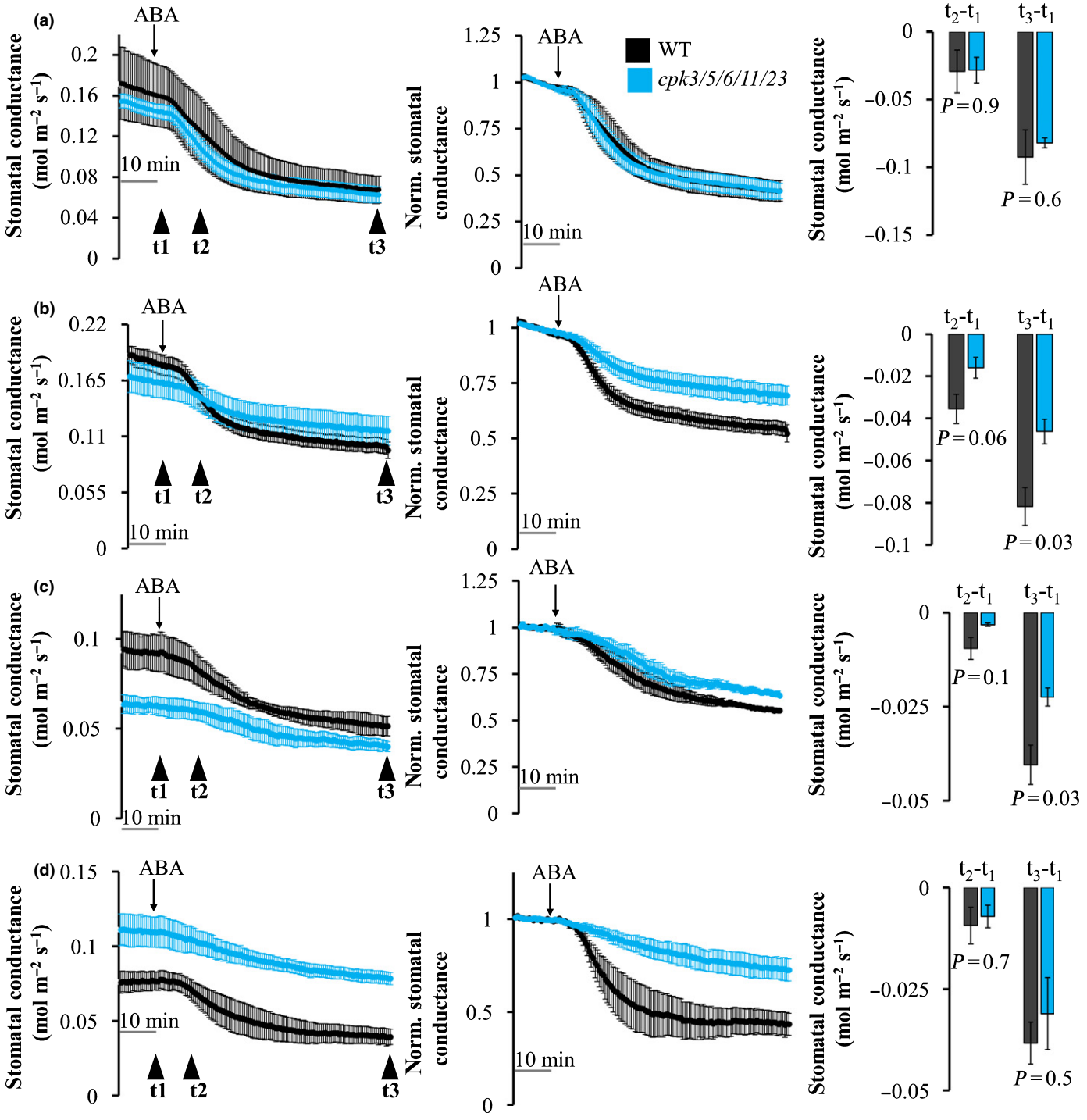

Fig. 7 Stomatal closure in response to abscisic acid (ABA) in leaves of *cpk3/5/6/11/23* quintuple mutants and wild-type (WT) plants. (a–d) Averaged time-resolved stomatal conductance responses (± SE) to 2 μM ABA analyzed in four independent experiments. ABA was added to the petiole of excised intact leaves of WT (Col-0) and *cpk3/5/6/11/23* quintuple mutant plants ((a) $n = 4$, (b) $n = 4$, (c) $n = 3$, and (d) $n = 4$ independent leaves per genotype). Stomatal conductance (left panels) was normalized to the average of the first 10 min of stomatal conductance values recorded (middle panels). Black downward pointing arrows indicate the application of ABA to the transpiration stream. Changes in absolute stomatal conductance are shown in the right panels. Differences in absolute stomatal conductance (mean ± SE) were calculated at the indicated time points (t_1, application of ABA; t_2, 10 min after application of ABA; t_3, final measurement). One-way ANOVA was used for statistical tests.

1996; Young *et al.*, 2006). Previous research has led to the model that elevated CO_2 enhances the Ca^{2+}-sensitivity of stomatal closing mechanisms as a CO_2-induced priming mechanism (Young *et al.*, 2006). However, the calcium-binding proteins that function in CO_2-dependent stomatal movements and their relative roles have remained unknown.

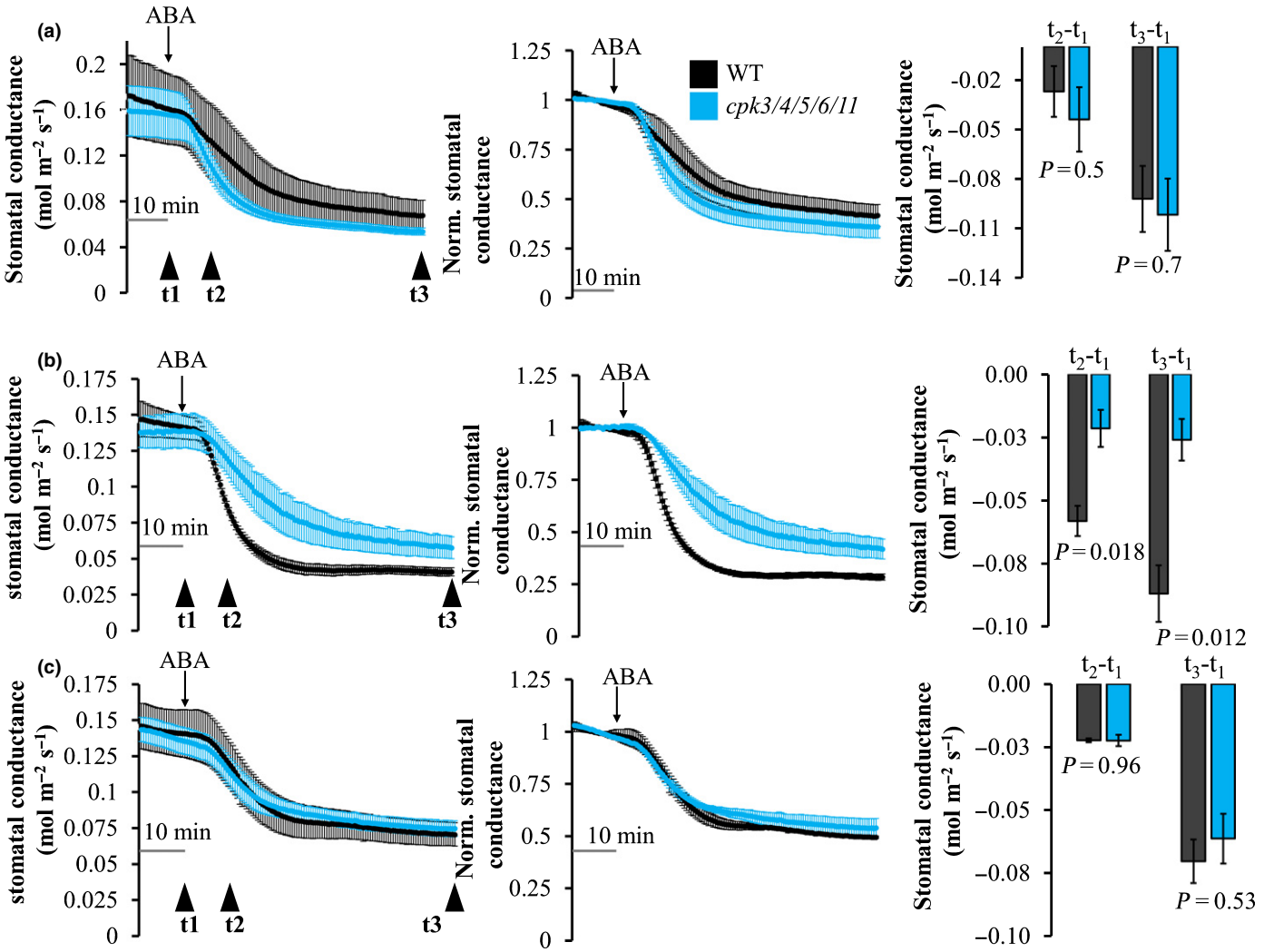

Fig. 8 Stomatal closure in response to abscisic acid (ABA) in leaves of *cpk3/4/5/6/11* quintuple mutants and wild-type plants. (a–c) Averaged time-resolved stomatal conductance responses (± SE) to 2 μM ABA analyzed in three independent experiments. ABA was added to the petiole of excised intact leaves of wild-type (WT, Col-0) and *cpk3/4/5/6/11* quintuple mutant plants ((a) $n = 4$, (b) $n = 3$, and (c) $n = 3$ independent leaves per genotype). Stomatal conductance (left panels) was normalized to the average of the first 10 min of stomatal conductance values recorded (middle panels). Black downward pointing arrows indicate the application of 2 μM ABA to the transpiration stream. Changes in absolute stomatal conductance are shown in the right panels. Differences in absolute stomatal conductance (mean ± SEM) were calculated at the indicated time points (t_1, application of ABA; t_2, 10 min after application of ABA; t_3, final measurement). One-way ANOVA was used for statistical tests.

Reversible elevation of guard cell $[Ca^{2+}]_{cyt}$ in response to elevated $[CO_2]$ suggested a correlation between $[CO_2]$ and calcium (Webb *et al.*, 1996). Ca^{2+} has been shown to contribute to stomatal closure mediated by CO_2 elevation, and elevated CO_2 increases cytosolic Ca^{2+} in *Commelina communis* guard cells (Schwartz *et al.*, 1988; Webb *et al.*, 1996). Young *et al.* (2006) further found rapid $[Ca^{2+}]_{cyt}$ transients that occurred at low $[CO_2]$. Moreover, elevated $[CO_2]$ was found to cause a slowing of repetitive $[Ca^{2+}]_{cyt}$ transients in Arabidopsis accession Landsberg *erecta* guard cells, which was attributed to high CO_2-induced depolarization of guard cells (Young *et al.*, 2006). Nevertheless, both low CO_2-induced stomatal opening and specifically an early phase of high CO_2-induced stomatal closing were both attenuated when Ca^{2+} elevations were inhibited (Young *et al.*, 2006).

CO_2- and light-induced stomatal movements in *cbl* and *cpk* mutant plants

Ca^{2+}-binding protein mutants that impair CO_2-regulated stomatal movements have not been identified to date. Thus, it is noteworthy that the findings of the present study demonstrate that both CO_2-mediated stomatal closure and opening were impaired in calcium-dependent protein kinase (CPK) *cpk3/5/6/11/23* quintuple mutants (Figs 2, S6). In recent years, it has been modeled that changing the kinetics of stomatal responses may affect crop performance, for example under varying light intensities (Deans *et al.*, 2019; Faralli *et al.*, 2019). In this respect, our present findings may provide additional mutants for new studies to test this model in a C_3 plant.

The Arabidopsis genome includes 34 CPK-encoding genes. Approximately 20 of these 34 CPKs are expressed in guard cells

at various levels, implicating concerted and possibly combinatorial functions during stomatal movements (Yip Delormel & Boudsocq, 2019). Unexpectedly, CO_2-mediated stomatal closing and opening were both impaired in *cpk3/5/6/11/23* quintuple mutant plants (Figs 2, S6). By contrast, *cpk5/6/11/23* quadruple and *cpk3/4/5/6/11* quintuple mutant plants exhibited wild-type-like CO_2 responses (Figs 1, S4). Different CPKs may have overlapping or partially overlapping functions at times, indicating genetic functional redundancy (Boudsocq & Sheen, 2013). The *cpk5/6/11/23* quadruple mutant showed intact CO_2-mediated stomatal closing responses in our assays (Fig. 1). By contrast, *cpk3/5/6/11/23* (Fig. 2) quintuple mutant leaves exhibited impaired stomatal responses, which could point to CPK3 being essential. However, *cpk3/4/5/6/11* quintuple mutant leaves showed intact responses to CO_2 (Fig. 1). This rather may be explained by a model in which the combination of cpk mutations crosses a threshold where the phenotype becomes visible.

Calcineurin B-like (CBL) proteins and the CBL-interacting protein kinases (CIPKs) that bind to CBL proteins can also affect stomatal responses (Luan *et al.*, 2002; Zhang *et al.*, 2014; Kudla *et al.*, 2018). For instance, *cbl1/cbl9* double mutant plants displayed enhanced stomatal closure in response to ABA treatment (Cheong *et al.*, 2007). Our data provide evidence that the five plasma membrane-targeted CBLs1, 4, 5, 8 and 9 (Batistič *et al.*, 2008, 2010; Chu *et al.*, 2021) are not substantially involved in CO_2-mediated stomatal movements, since *cbl1/4/5/8/9* quintuple mutant plants did not show clear and substantial altered stomatal response kinetics to shifts in $[CO_2]$, although the amplitude of the stomatal closing response may have been reduced in one experimental set (Fig. 4).

An important question arises from previous stomatal response studies and the present study: how can Ca^{2+} and indeed CPKs function in two distinct responses (CO_2-controlled stomatal closing and stomatal opening)? Previous research in guard cells has shown that the biological stimuli – elevated CO_2 and ABA– prime (i.e. enhance) the Ca^{2+} sensitivity of S-type anion channel activation that functions in stomatal closing (Young *et al.*, 2006; Siegel *et al.*, 2009; Chen *et al.*, 2010; Brandt *et al.*, 2015). A biochemical mechanism for this stimulus-induced Ca^{2+} sensitivity priming has been identified in ABA signaling (Brandt *et al.*, 2015). Additional nonexclusive models have been investigated in which the spatiotemporal pattern of Ca^{2+} elevations encodes information that can transmit a specific response to Ca^{2+} (McAinsh *et al.*, 1992; Knight *et al.*, 1996; Knight & Knight, 2000; Hetherington & Brownlee, 2004; Dodd *et al.*, 2010). The present findings suggest that CO_2 signaling analyses of the isolated *cpk3/5/6/11/23* quintuple mutant could provide a potent model system for dissection of mechanisms mediating specificity in Ca^{2+} signaling.

During stomatal opening, K^+_{in} channels contribute to K^+ uptake driven by plasma membrane H^+-ATPases in guard cells (Kwak *et al.*, 2001; Lebaudy *et al.*, 2008). Inward rectifying K^+ channel activity was decreased in *cpk3/5/6/11/23* quintuple mutant guard cells (Fig. 5). $[Ca^{2+}]_{cyt}$ functions as a negative regulator of guard cell K^+_{in} channels (Schroeder & Hagiwara, 1989; Grabov & Blatt, 1999). Similar reductions in K^+_{in} current magnitudes were previously observed when K^+_{in} channel activity was genetically repressed via dominant negative KAT1 expression or indirectly downregulated in *slac1* (SLOW ANION CHANNEL 1) mutant plants (Kwak *et al.*, 2001; Laanemets *et al.*, 2013). Similar to *cpk3/5/6/11/23* quintuple mutants, *slac1* mutant plants also displayed defective stomatal closing at high CO_2; interestingly, however, they also exhibited a slowed low CO_2-induced stomatal opening (Negi *et al.*, 2008; Vahisalu *et al.*, 2008; Laanemets *et al.*, 2013). Of additional interest is the observation that mutating a residue in SLAC1 that is required for bicarbonate upregulation of S-type anion channel activity also led to slowing of both CO_2-mediated stomatal opening and closing, but did not abrogate ABA-induced stomatal closing (Zhang *et al.*, 2018a,b).

Notably, light-induced stomatal opening was slowed in *slac1* (Laanemets *et al.*, 2013) but not in *cpk3/5/6/11/23* quintuple mutant plants (Figs 6, S7). This raises a question for the present study: why was stomatal opening triggered by low $[CO_2]$ impaired, but not stomatal opening triggered by red light and blue light? These findings suggest that additional mechanisms other than K^+_{in} channel regulation are likely to be affected in the *cpk3/5/6/11/23* quintuple mutant. Previous research showed that K^+_{in} channel downregulation by 70% alone, similar to the average *c.* 60–69% reduction found here (Fig. 5), would not substantially slow physiological rates of K^+ uptake during stomatal opening (Kwak *et al.*, 2001). Residual 30% K^+_{in} channel activity has been found to be sufficient for wild-type-like stomatal opening (Kwak *et al.*, 2001). Therefore, it is likely that mutations in *cpk3/5/6/11/23* affect additional mechanisms – for example, proton pump activity in response to low CO_2 may be affected. Current knowledge on crosstalk between light and CO_2 specifically in regulation of plasma membrane H^+-ATPases is still limited. It was hypothesized that high $[CO_2]$ might inhibit plasma membrane (PM) H^+-ATPase activity (Edwards & Bowling, 1985). However, low $[CO_2]$ conditions did not induce phosphorylation of PM H^+-ATPase in the dark (Ando & Kinoshita, 2018). The slowed stomatal opening kinetics and the reduced K^+_{in} channel activity observed in the *cpk3/5/6/11/23* quintuple mutant have also been found in *slac1* mutant alleles (Laanemets *et al.*, 2013). In the case of *slac1* mutant alleles, which are mainly impaired in stomatal closing responses, previous research has suggested that the slowed stomatal opening can be explained by Ca^{2+}-dependent compensatory effects of *slac1* mutation on stomatal opening mechanisms (Laanemets *et al.*, 2013).

ABA-mediated stomatal closure in *cpk3/4/5/6/11* and *cpk3/5/6/11/23* quintuple mutants

ABA-dependent stomatal closing was slightly impaired in *cpk3/6* and *cpk5/6/11/23* quadruple mutant plants in stomatal aperture assays (Mori *et al.*, 2006; Brandt *et al.*, 2015) and strongly affected in *cpk4/11* double mutants (Zhu *et al.*, 2007). When the ABA concentration was increased to 10 μM, stomata of *cpk5/6/11/23* quadruple mutant plants showed ABA responsiveness, indicating that this *cpk* mutant phenotype can be bypassed (Brandt *et al.*, 2015). Abscisic acid-induced stomatal closure was

not affected in a distinct quadruple mutant, *cpk3/5/6/11* (Guzel Deger *et al.*, 2015). The present study suggests that variable and/or partial impairment and slowing in stomatal closing mediated by 2 μM or 0.7 μM ABA in intact leaves of *cpk3/5/6/11/23* quintuple mutant plants, since responses ranged from largely intact in some experiments to slowed and slightly impaired stomatal closing in other independent experimental sets (Figs 7, S8). Similar variable ABA-mediated stomatal closing responses were obtained during analyses in leaves of *cpk3/4/5/6/11* quintuple mutant plants. Although only one of a total of three independent experiment sets showed slightly impaired 2 μM ABA-induced stomatal closure in leaves of *cpk3/4/5/6/11* quintuple mutants (Fig. 8), application of 0.7 μM ABA to the transpiration stream of *cpk3/4/5/6/11* quintuple mutant leaves induced variable amplitudes in stomatal closing in three experimental sets and was partially slower in one of three independent experimental data sets (Fig. S9). In the present study, time-resolved stomatal conductance changes were analyzed during application of ABA to the petiole of excised intact leaves. Previous studies measured stomatal apertures in excised intact leaves which were floated on stomatal opening buffer for 2–2.5h before application of ABA (Mori *et al.*, 2006; Zhu *et al.*, 2007). Differences in the observed phenotypes between stomatal aperture measurements and time-resolved stomatal conductance measurements in intact leaves have been discussed previously (Ceciliato *et al.*, 2019). Note that in the present study, the ABA concentration at the guard cells should be much higher than at the petiole, since water evaporates at stomata and the transpiration stream had a substantial conductance. This may contribute to the difference between stomatal measurements made in isolated leaves and intact leaves, given that a higher ABA concentration was previously found to partially bypass the stomatal response in *cpk* mutant epidermides (Brandt *et al.*, 2015). Such a concentration-dependent effect is not of concern for the exposure of intact leaves to changes in CO_2 concentration and light. Interestingly, in previous studies ABA regulation of S-type anion channels in *cpk5/6/11/23* quadruple mutant plants and Ca^{2+} activation of S-type anion channels in *cpk23* single mutant plants (Geiger *et al.*, 2010) was more strongly affected than ABA-induced stomatal closing (Brandt *et al.*, 2015). Together with the present study, these data suggest that additional channels and transporters that function in stomatal movements may include important CPK-independent mechanisms, as ABA-induced stomatal closing is mediated by a network of regulated ion channels and transporters in the plasma membrane and vacuolar membrane of guard cells (Albert *et al.*, 2017). R-type (QUAC1) anion channels function in parallel to S-type anion channels (Keller *et al.*, 1989), and the amplitude of R-type anion channels was not affected in *cpk3/cpk6* double mutant guard cells (Mori *et al.*, 2006). Further research into *in planta* regulation of other guard cell ion channels and transporters in higher order *cpk* mutants could elucidate bypass mechanisms.

Recent Boolean modeling studies have suggested that Ca^{2+} may affect the rate of ABA-induced stomatal movements (Albert *et al.*, 2017; Waidyarathne & Samarasinghe, 2018). Previous research has showed that ABA signaling could proceed when Ca^{2+} elevations were abolished in guard cells (Siegel *et al.*, 2009). However, the ABA response was clearly slowed and attenuated when cytosolic Ca^{2+} elevations were fully abolished (Siegel *et al.*, 2009). In line with these findings, ABA-induced stomatal closing was slower in guard cells when cytosolic Ca^{2+} transients were absent (Huang *et al.*, 2019). Whether higher order mutants in Ca^{2+} binding proteins can further weaken the ABA response remains to be determined. Interestingly however, in the present study the high CO_2 response was more clearly slowed than the ABA response, indicating that CPKs have a prominent role in the CO_2 response.

Conclusions

In summary, the present study reveals important insights into a crucial function of CPKs in CO_2-controlled stomatal movements. The combinatorial knockout of *cpk3/5/6/11/23* caused a clear slowing of high CO_2-induced stomatal closing. We also reveal that *cpk3/5/6/11/23* quintuple mutant plants showed a slowed low CO_2-induced stomatal opening response. By contrast, red light- and blue light-induced stomatal opening was not clearly impaired in *cpk3/5/6/11/23* quintuple mutant plants under the imposed conditions.

The presented findings further support the model that the *c.* 60–69% reduced activity in K^+_{in} channel current magnitudes, as found in *cpk3/5/6/11/23* quintuple mutant guard cells, is not on its own sufficient to slow physiological stomatal opening by light stimuli, in line with previous findings (Kwak *et al.*, 2001). Therefore, in *cpk3/5/6/11/23* quintuple mutant guard cells, it is likely that additional mechanisms contribute to the slowed low CO_2-induced stomatal opening. It would be interesting to analyze parallel mechanisms, including R-type anion channels and other mechanisms in *cpk3/5/6/11/23* quintuple mutant guard cells, that could provide sufficient bypass anion efflux to limit regulation effects of the *cpk3/5/6/11/23* quintuple mutant on S-type anion channels. Analyses of ABA responses in the present study correlate with recent models and studies suggesting a modulation and acceleration of the ABA response by Ca^{2+}. The findings of the present study further demonstrate that a quintuple mutant in the five plasma membrane-targeted CBL proteins, CBL1, 4, 5, 8 and 9, did not affect the kinetics of CO_2-regulated stomatal closing and opening in intact plant leaves. The variability of the ABA response in intact leaves of *cpk* quintuple mutant plants presented here and in previous analyses supports the model that Ca^{2+} can play an accelerating role in stomatal ABA signaling. Higher order Ca^{2+}-binding protein mutants may be needed to further investigate this hypothesis in intact plant leaves. Additional research will be needed to identify protein targets whose phosphorylation-dependent regulation is affected by CO_2 in *cpk3/5/6/11/23* quintuple mutant guard cells.

Acknowledgements

This research was funded by a grant from the National Science Foundation (MCB-1900567) and in part by the National Institutes of Health (GM060396-ES010337) to JIS. SS was supported by a Deutsche Forschungsgemeinschaft (DFG) fellowship

(SCHU 3186/1-1:1). PHOC was supported by a CNPq scholarship from Brazil (203406/2014-1). SM was supported by a Fund for the Promotion of Joint International Research (Fostering Joint International Research (A)) grant (18KK0425) from the Japan Society for the Promotion of Science (JSPS). GD was supported by an EMBO long-term postdoctoral fellowship (ALTF334-2018). TA-S was supported by a postdoctoral fellowship from the US-Israel Binational Agricultural Research and Development Fund (BARD F1-446-11). Research in HK's group was supported by the Estonian Research Council (PRG433, PRG719) and European Regional Development Fund (Center of Excellence in Molecular Cell Engineering CEMCE). Research in JK's group was supported by grants from the DFG (Ku931/8-3i, 615410). We thank Dr. Jingbo Zhang and Thomas Belknap for technical support and assistance with genotyping and with the generation of *cpk* quintuple mutant plants, respectively.

Author contributions

This study was designed by JIS, SS, TA-S and HK. SS, MN, DY and PHOC performed stomatal conductance analyses. SM conducted patch clamp experiments with guard cells. Stomatal density assays were carried out by RD and JA. GD conducted curve-fitting analyses. LS, JNO and JK generated the *cbl* quintuple mutant. JIS and SS wrote the manuscript with comments from all authors.

ORCID

Tamar Azoulay-Shemer https://orcid.org/0000-0002-4291-6901
Paulo H. O. Ceciliato https://orcid.org/0000-0002-9729-9429
Guillaume Dubeaux https://orcid.org/0000-0003-0275-8467
Hannes Kollist https://orcid.org/0000-0002-6895-3583
Jörg Kudla https://orcid.org/0000-0002-8238-767X
Shintaro Munemasa https://orcid.org/0000-0003-1204-1822
Maris Nuhkat https://orcid.org/0000-0002-8001-4220
Julian I. Schroeder https://orcid.org/0000-0002-3283-5972
Sebastian Schulze https://orcid.org/0000-0001-8000-0577
Leonie Steinhorst https://orcid.org/0000-0002-1592-2732
Dmitry Yarmolinsky https://orcid.org/0000-0002-9372-6091

References

Albert R, Acharya BR, Jeon BW, Zañudo JGT, Zhu M, Osman K, Assmann SM. 2017. A new discrete dynamic model of ABA-induced stomatal closure predicts key feedback loops. *PLoS Biology* **15**: e2003451.

Albrecht V, Weinl S, Blazevic D, D'Angelo C, Batistič O, Kolukisaoglu Ü, Bock R, Schulz B, Harter K, Kudla J. 2003. The calcium sensor CBL1 integrates plant responses to abiotic stresses. *The Plant Journal* **36**: 457–470.

Ando E, Kinoshita T. 2018. Red light-induced phosphorylation of plasma membrane H^+-ATPase in stomatal guard cells. *Plant Physiology* **178**: 838–849.

Assmann SM, Shimazaki KI. 1999. The multisensory guard cell. Stomatal responses to blue light and abscisic acid. *Plant Physiology* **119**: 809–815.

Azoulay-Shemer T, Palomares A, Bagheri A, Israelsson-Nordstrom M, Engineer CB, Bargmann BOR, Stephan AB, Schroeder JI. 2015. Guard cell photosynthesis is critical for stomatal turgor production, yet does not directly mediate CO_2- and ABA-induced stomatal closing. *The Plant Journal* **83**: 567–581.

Batistič O, Kudla J. 2009. Plant calcineurin B-like proteins and their interacting protein kinases. *Biochimica et Biophysica Acta – Molecular Cell Research* **1793**: 985–992.

Batistič O, Sorek N, Schültke S, Yalovsky S, Kudla J. 2008. Dual fatty acyl modification determines the localization and plasma membrane targeting of CBL/CIPK Ca^{2+} signaling complexes in Arabidopsis. *Plant Cell* **20**: 1346–1362.

Batistič O, Waadt R, Steinhorst L, Held K, Kudla J. 2010. CBL-mediated targeting of CIPKs facilitates the decoding of calcium signals emanating from distinct cellular stores. *The Plant Journal* **61**: 211–222.

Boudsocq M, Sheen J. 2013. CDPKs in immune and stress signaling. *Trends in Plant Science* **18**: 30–40.

Boudsocq M, Willmann MR, McCormack M, Lee H, Shan L, He P, Bush J, Cheng SH, Sheen J. 2010. Differential innate immune signalling via Ca^{2+} sensor protein kinases. *Nature* **464**: 418–422.

Brandt B, Munemasa S, Wang C, Nguyen D, Yong T, Yang PG, Poretsky E, Belknap TF, Waadt R, Alemań F *et al.* 2015. Calcium specificity signaling mechanisms in abscisic acid signal transduction in Arabidopsis guard cells. *eLife* **4**: 1–25.

Ceciliato PHO, Zhang J, Liu Q, Shen X, Hu H, Liu C, Schäffner AR, Schroeder JI. 2019. Intact leaf gas exchange provides a robust method for measuring the kinetics of stomatal conductance responses to abscisic acid and other small molecules in and grasses. *Plant Methods* **15**: 38.

Chen DH, Liu HP, Li CL. 2019. Calcium-dependent protein kinase CPK9 negatively functions in stomatal abscisic acid signaling by regulating ion channel activity in Arabidopsis. *Plant Molecular Biology* **99**: 113–122.

Chen ZH, Hills A, Lim CK, Blatt MR. 2010. Dynamic regulation of guard cell anion channels by cytosolic free Ca^{2+} concentration and protein phosphorylation. *The Plant Journal* **61**: 816–825.

Cheng SH, Willmann MR, Chen HC, Sheen J. 2002. Calcium signaling through protein kinases. The Arabidopsis calcium-dependent protein kinase gene family. *Plant Physiology* **129**: 469–485.

Cheong YH, Pandey GK, Grant JJ, Batistic O, Li L, Kim B-G, Lee S-C, Kudla J, Luan S. 2007. Two calcineurin B-like calcium sensors, interacting with protein kinase CIPK23, regulate leaf transpiration and root potassium uptake in Arabidopsis. *The Plant Journal* **52**: 223–239.

Chu L-CC, Offenborn JN, Steinhorst L, Wu XN, Lin X, Li Z, Jacquot A, Lejay L, Kudla J, Schulze WX. 2021. Plasma membrane CBL Ca^{2+} sensor proteins function in regulating primary root growth and nitrate uptake by affecting global phosphorylation patterns and microdomain protein distribution. *New Phytologist* **229**: 2223–2237.

Cousson A, Vavasseur A. 1998. Putative involvement of cytosolic Ca^{2+} and GTP-binding proteins in cyclic-GMP-mediated induction of stomatal opening by auxin in *Commelina communis* L. *Planta* **206**: 308–314.

De Silva DLR, De Cox RC, Hetherington AM, Mansfield TA. 1985. Suggested involvement of calcium and calmodulin in the responses of stomata to abscisic acid. *New Phytologist* **101**: 555–563.

Deans RM, Brodribb TJ, Busch FA, Farquhar GD. 2019. Plant water-use strategy mediates stomatal effects on the light induction of photosynthesis. *New Phytologist* **222**: 382–395.

Dodd AN, Kudla J, Sanders D. 2010. The language of calcium signaling. *Annual Review of Plant Biology* **61**: 593–620.

Edwards A, Bowling DJF. 1985. Evidence for a CO_2 inhibited proton extrusion pump in the stomatal cells of *Tradescantia virginiana*. *Journal of Experimental Botany* **36**: 91–98.

Faralli M, Matthews J, Lawson T. 2019. Exploiting natural variation and genetic manipulation of stomatal conductance for crop improvement. *Current Opinion in Plant Biology* **49**: 1–7.

Geiger D, Scherzer S, Mumm P, Marten I, Ache P, Matschi S, Liese A, Wellmann C, Al-Rasheid KAS, Grill E *et al.* 2010. Guard cell anion channel SLAC1 is regulated by CDPK protein kinases with distinct Ca^{2+} affinities. *Proceedings of the National Academy of Sciences, USA* **107**: 8023–8028.

Gobert A, Isayenkov S, Voelker C, Czempinski K, Maathuis FJM. 2007. The two-pore channel *TPK1* gene encodes the vacuolar K^+ conductance and plays a

role in K^+ homeostasis. *Proceedings of the National Academy of Sciences, USA* **104**: 10726–10731.

Grabov A, Blatt MR. 1997. Parallel control of the inward-rectifier K^+ channel by cytosolic free Ca^{2+} and pH *Vicia* guard cells. *Planta* **201**: 84–95.

Grabov A, Blatt MR. 1998. Membrane voltage initiates Ca^{2+} waves and potentiates Ca^{2+} increases with abscisic acid in stomatal guard cells. *Proceedings of the National Academy of Sciences, USA* **95**: 4778–4783.

Grabov A, Blatt MR. 1999. A steep dependence of inward-rectifying potassium channels on cytosolic free calcium concentration increase evoked by hyperpolarization in guard cells. *Plant Physiology* **119**: 277–287.

Guzel Deger A, Scherzer S, Nuhkat M, Kedzierska J, Kollist H, Brosché M, Unyayar S, Boudsocq M, Hedrich R, Roelfsema MRG. 2015. Guard cell SLAC1-type anion channels mediate flagellin-induced stomatal closure. *New Phytologist* **208**: 162–173.

Hauser F, Ceciliato PHO, Lin YC, Guo DD, Gregerson JD, Abbasi N, Youhanna D, Park J, Dubeaux G, Shani E *et al.* 2019. A seed resource for screening functionally redundant genes and isolation of new mutants impaired in CO_2 and ABA responses. *Journal of Experimental Botany* **70**: 641–651.

Hetherington AM, Brownlee C. 2004. The generation of Ca^{2+} signals in plants. *Annual Review of Plant Biology* **55**: 401–427.

Huang S, Waadt R, Nuhkat M, Kollist H, Hedrich R, Roelfsema MRG. 2019. Calcium signals in guard cells enhance the efficiency by which abscisic acid triggers stomatal closure. *New Phytologist* **224**: 177–187.

Keller BU, Hedrich R, Raschke K. 1989. Voltage-dependent anion channels in the plasma membrane of guard cells. *Nature* **341**: 450–453.

Kinoshita T, Nishimura M, Shimazaki KI. 1995. Cytosolic concentration of Ca^{2+} regulates the plasma membrane H^+-ATPase in guard cells of fava bean. *Plant Cell* **7**: 1333–1342.

Knight H, Knight MR. 2000. Imaging spatial and cellular characteristics of low temperature calcium signature after cold acclimation in Arabidopsis. *Journal of Experimental Botany* **51**: 1679–1686.

Knight H, Trewavas AJ, Knight MR. 1996. Cold calcium signaling in Arabidopsis involves two cellular pools and a change in calcium signature after acclimation. *Plant Cell* **8**: 489–503.

Kollist H, Nuhkat M, Roelfsema MRG. 2014. Closing gaps: linking elements that control stomatal movement. *New Phytologist* **203**: 44–62.

Kollist T, Moldau H, Rasulov B, Oja V, Rämma H, Hüve K, Jaspers P, Kangasjärvi J, Kollist H. 2007. A novel device detects a rapid ozone-induced transient stomatal closure in intact Arabidopsis and its absence in *abi2* mutant. *Physiologia Plantarum* **129**: 796–803.

Kudla J, Becker D, Grill E, Hedrich R, Hippler M, Kummer U, Parniske M, Romeis T, Schumacher K. 2018. Advances and current challenges in calcium signaling. *New Phytologist* **218**: 414–431.

Kudla J, Xu Q, Harter K, Gruissem W, Luan S. 1999. Genes for calcineurin B-like proteins in Arabidopsis are differentially regulated by stress signals. *Proceedings of the National Academy of Sciences, USA* **96**: 4718–4723.

Kwak JM, Murata Y, Baizabal-Aguirre VM, Merrill J, Wang M, Kemper A, Hawke SD, Tallman G, Schroeder JI. 2001. Dominant negative guard cell K^+ channel mutants reduce inward-rectifying K^+ currents and light-induced stomatal opening in Arabidopsis. *Plant Physiology* **127**: 473–485.

Laanemets K, Wang YF, Lindgren O, Wu J, Nishimura N, Lee S, Caddell D, Merilo E, Brosche M, Kilk K *et al.* 2013. Mutations in the SLAC1 anion channel slow stomatal opening and severely reduce K^+ uptake channel activity via enhanced cytosolic $[Ca^{2+}]$ and increased Ca^{2+} sensitivity of K^+ uptake channels. *New Phytologist* **197**: 88–98.

Lebaudy A, Vavasseur A, Hosy E, Dreyer I, Leonhardt N, Thibaud JB, Véry AA, Simonneau T, Sentenac H. 2008. Plant adaptation to fluctuating environment and biomass production are strongly dependent on guard cell potassium channels. *Proceedings of the National Academy of Sciences, USA* **105**: 5271–5276.

Li Z, Takahashi Y, Scavo A, Brandt B, Nguyen D, Rieu P, Schroeder JI. 2018. Abscisic acid-induced degradation of Arabidopsis guanine nucleotide exchange factor requires calcium-dependent protein kinases. *Proceedings of the National Academy of Sciences, USA* **115**: E4522–E4531.

Liu KH, Niu Y, Konishi M, Wu Y, Du H, Sun Chung H, Li L, Boudsocq M, McCormack M, Maekawa S *et al.* 2017. Discovery of nitrate-CPK-NLP signalling in central nutrient-growth networks. *Nature* **545**: 311–316.

Luan S, Kudla J, Rodriguez-Concepcion M, Yalovsky S, Gruissem W. 2002. Calmodulins and calcineurin B-like proteins: calcium sensors for specific signal response coupling in plants. *Plant Cell* **14**: S389–S400.

MacRobbie EAC. 2000. ABA activates multiple Ca^{2+} fluxes in stomatal guard cells, triggering vacuolar K^+ (Rb) release. *Proceedings of the National Academy of Sciences, USA* **97**: 12361–12368.

Mao J, Manik SMN, Shi S, Chao J, Jin Y, Wang Q, Liu H. 2016. Mechanisms and physiological roles of the CBL-CIPK networking system in *Arabidopsis thaliana*. *Genes* **7**: 62.

McAinsh MR, Brownlee C, Hetherington AM. 1990. Abscisic acid-induced elevation of guard cell cytosolic Ca^{2+} precedes stomatal closure. *Nature* **343**: 186–188.

McAinsh MR, Brownlee C, Hetherington AM. 1992. Visualizing changes in cytosolic-free Ca^{2+} during the response of stomatal guard cells to abscisic acid. *Plant Cell* **4**: 1113–1122.

Mori IC, Murata Y, Yang Y, Munemasa S, Wang YF, Andreoli S, Tiriac H, Alonso JM, Harper JF, Ecker JR *et al.* 2006. CDPKs CPK6 and CPK3 function in ABA regulation of guard cell S-type anion- and Ca^{2+}- permeable channels and stomatal closure. *PLoS Biology* **4**: 1749–1762.

Mott KA. 1988. Do stomata respond to CO_2 concentrations other than intercellular? *Plant Physiology* **86**: 200–203.

Murata Y, Mori IC, Munemasa S. 2015. Diverse stomatal signaling and the signal integration mechanism. *Annual Review of Plant Biology* **66**: 369–392.

Negi J, Matsuda O, Nagasawa T, Oba Y, Takahashi H, Kawai-Yamada M, Uchimiya H, Hashimoto M, Iba K. 2008. CO_2 regulator SLAC1 and its homologues are essential for anion homeostasis in plant cells. *Nature* **452**: 483–486.

Pandey GK, Yong HC, Kim KN, Grant JJ, Li L, Hung W, D'Angelo C, Weinl S, Kudla J, Luan S. 2004. The calcium sensor calcineurin B-like 9 modulates abscisic acid sensitivity and biosynthesis in Arabidopsis. *Plant Cell* **16**: 1912–1924.

Reddy ASN, Ali GS, Celesnik H, Day IS. 2011. Coping with stresses: roles of calcium- and calcium/calmodulin-regulated gene expression. *Plant Cell* **23**: 2010–2032.

Schroeder JI, Hagiwara S. 1989. Cytosolic calcium regulates ion channels in the plasma membrane of *Vicia faba* guard cells. *Nature* **338**: 427–430.

Schwartz A. 1985. Role of Ca^{2+} and EGTA on stomatal movements in *Commelina communis* L. *Plant Physiology* **79**: 1003–1005.

Schwartz A, Ilan N, Grantz DA. 1988. Calcium effects on stomatal movement in *Commelina communis* L. *Plant Physiology* **87**: 583–587.

Shao J, Harmon AC. 2003. *In vivo* phosphorylation of a recombinant peptide substrate of CDPK suggests involvement of CDPK in plant stress responses. *Plant Molecular Biology* **53**: 691–700.

Sheen J. 1996. Ca^{2+}-dependent protein kinases and stress signal transduction in plants. *Science* **274**: 1900–1902.

Shimazaki K, Doi M, Assmann SM, Kinoshita T. 2007. Light regulation of stomatal movement. *Annual Review of Plant Biology* **58**: 219–247.

Shimazaki KI, Kinoshita T, Nishimura M. 1992. Involvement of calmodulin and calmodulin-dependent myosin light chain kinase in blue light-dependent H^+ pumping by guard cell protoplasts from *Vicia faba* L. *Plant Physiology* **99**: 1416–1421.

Siegel RS, Xue S, Murata Y, Yang Y, Nishimura N, Wang A, Schroeder JI. 2009. Calcium elevation-dependent and attenuated resting calcium-dependent abscisic acid induction of stomatal closure and abscisic acid-induced enhancement of calcium sensitivities of S-type anion and inward-rectifying K^+ channels in Arabidopsis guard cells. *The Plant Journal* **59**: 207–220.

Vahisalu T, Kollist H, Wang Y-F, Nishimura N, Chan W-Y, Valerio G, Lamminmäki A, Brosché M, Moldau H, Desikan R *et al.* 2008. SLAC1 is required for plant guard cell S-type anion channel function in stomatal signalling. *Nature* **452**: 487–491.

Waidyarathne P, Samarasinghe S. 2018. Boolean calcium signalling model predicts calcium role in acceleration and stability of abscisic acid-mediated stomatal closure. *Scientific Reports* **8**: 1–16.

Ward JM, Schroeder JI. 1994. Calcium-activated K^+ channels and calcium-induced calcium release by slow vacuolar ion channels in guard cell vacuoles implicated in the control of stomatal closure. *Plant Cell* **6**: 669–683.

Webb AAR, McAinsh MR, Mansfield TA, Hetherington AM. 1996. Carbon dioxide induces increases in guard cell cytosolic free calcium. *The Plant Journal* **9**: 297–304.

Yip Delormel T, Boudsocq M. 2019. Properties and functions of calcium-dependent protein kinases and their relatives in *Arabidopsis thaliana*. *New Phytologist* **224**: 585–604.

Young JJ, Mehta S, Israelsson M, Godoski J, Grill E, Schroeder JI. 2006. CO_2 signaling in guard cells: calcium sensitivity response modulation, a Ca^{2+}-independent phase, and CO_2 insensitivity of the *gca2* mutant. *Proceedings of the National Academy of Sciences, USA* **103**: 7506–7511.

Zhang H, Liu D, Yang B, Liu WZ, Mu B, Song H, Chen B, Li Y, Ren D, Deng H *et al.* 2020. Arabidopsis CPK6 positively regulates ABA signaling and drought tolerance through phosphorylating ABA-responsive element-binding factors. *Journal of Experimental Botany* **71**: 188–203.

Zhang J, De-oliveira-Ceciliato P, Takahashi Y, Schulze S, Dubeaux G, Hauser F, Azoulay-Shemer T, Tõldsepp K, Kollist H, Rappel WJ *et al.* 2018a. Insights into the molecular mechanisms of CO_2-Mediated Regulation of Stomatal Movements. *Current Biology* **28**: R1356–R1363.

Zhang J, Wang N, Miao Y, Hauser F, McCammon JA, Rappel WJ, Schroeder JI. 2018b. Identification of SLAC1 anion channel residues required for CO_2/bicarbonate sensing and regulation of stomatal movements. *Proceedings of the National Academy of Sciences, USA* **115**: 11129–11137.

Zhang T, Chen S, Harmon AC. 2014. Protein phosphorylation in stomatal movement. *Plant Signaling and Behavior* **9**: e972845.

Zhu SY, Yu XC, Wang XJ, Zhao R, Li Y, Fan RC, Shang Y, Du SY, Wang XF, Wu FQ *et al.* 2007. Two calcium-dependent protein kinases, CPK4 and CPK11, regulate abscisic acid signal transduction in Arabidopsis. *Plant Cell* **19**: 3019–3036.

Supporting Information

Additional Supporting Information may be found online in the Supporting Information section at the end of the article.

Fig. S1 Curve fitting and statistical analyses of the amplitude and time constant (τ) values for wild-type (WT) and *cpk5/6/11/23* quadruple mutant plants in gas exchange experiments presented in Fig. 1(a).

Fig. S2 Genotyping of *cpk3/4/5/6/11*, *cpk3/5/6/11/23* quintuple mutant plants and *cpk5/6/11/23* quadruple mutant plants.

Fig. S3 Curve fitting and statistical analyses of the amplitude and time constant (τ) values for WT and *cpk3/4/5/6/11* quintuple mutant plants in the gas exchange experiments presented in Fig. 1(c).

Fig. S4 Independent experiments showing stomatal conductance in intact whole plant rosettes of *cpk3/5/6/11/23* and *cpk3/4/5/6/11* quintuple mutants in response to shifts in air CO_2 concentrations, as measured independently in whole intact rosettes of Arabidopsis.

Fig. S5 Curve fitting and statistical analyses of the amplitude and time constant (τ) values for WT and *cpk3/5/6/11/23* quintuple mutant plants in the gas exchange experiments presented in Fig. 2(a).

Fig. S6 Independent experimental data set showing that stomatal opening and closure responses to shifts in ambient CO_2 concentrations are altered in leaves of intact *cpk3/5/6/11/23* quintuple mutant plants.

Fig. S7 Independent experiment example showing that guard cells of *cpk3/5/6/11/23* quintuple mutant leaves are not impaired in red light and blue light-induced stomatal opening.

Fig. S8 Stomatal closure in response to 0.7 μM ABA in leaves of *cpk3/5/6/11/23* quintuple mutants and WT plants.

Fig. S9 0.7 μM ABA-mediated stomatal closure in intact leaves of *cpk3/4/5/6/11* quintuple mutant and WT plants.

Table S1 Oligonucleotides used for genotyping of *cpk* mutant lines.